Polarization forces in collisions between low-energy electrons and sodium clusters

V. Kasperovich, G. Tikhonov, K. Wong, P. Brockhaus, and V. V. Kresin

Department of Physics and Astronomy, University of Southern California, Los Angeles, California 90089-0484

We study low-energy ($E \sim 0-5$ eV) electron collisions with free neutral Na_n clusters ($n = 20,40,57,58,70$). The measured inelastic cross sections range from several hundred Å^2 at $E > 1$ eV up to well over a thousand Å^2 for $E \rightarrow 0$, signifying the action of strong long-range polarization forces. For collision energies below 1 eV, the cross sections rise strongly with decreasing energy, and are in good agreement with values predicted by the mechanism of electron capture by the polarization field of the cluster. At higher energies, the cross sections become approximately independent of the collision energy, implying efficient energy transfer at large impact parameters. This may proceed via excitation of collective and single-particle resonances of the cluster electron cloud by the incoming electron, followed by fragmentation. [S1050-2947(99)02910-8]

PACS number(s): 36.40.−c, 34.80.Ht

I. INTRODUCTION

Clusters of alkali-metal atoms are highly polarizable [1–4], which leads to the appearance of strong long-range forces in cluster interactions. Examples include the dispersion van der Waals attraction manifested in elastic scattering of clusters off neutral atoms and molecules [5,6], the polarization force arising in cluster collisions with fast ions [7], and the polarization interaction between fragments in cluster fission [8]. In this paper we report on another long-range interaction effect involving metal clusters: an observation of large cross sections for inelastic collisions of slow electrons with neutral sodium clusters. As discussed below, we propose that these cross sections reflect electron capture by the polarization field for impact energies $E < 1$ eV. For higher energies, the dominant inelastic channel is collision-induced fragmentation (possibly proceeding via intermediate electronic excitations of the cluster).

Low-energy capture of free electrons by molecules has been studied extensively (see, e.g., the reviews [9–12]), but similar experiments on free clusters have been primarily limited to molecular clusters [10,13–15] and fullerenes [10,16–21]. Information on metallic clusters is very limited. An earlier experiment on Na_n ($n = 8,20,40$) [22] indicated the presence of large electron scattering cross sections and suggested an interpretation in terms of attachment and fragmentation processes. However, due to the low signal-to-noise quality it remained uncertain whether the cross sections truly displayed a strong rise for $E \rightarrow 0$, which is a signature of electron attachment. A number of theoretical papers have subsequently addressed the issue of inelastic low- and medium-energy electron collisions with metal clusters, discussing various energy loss mechanisms: single-electron transitions, excitation of collective oscillations, emission of radiation, and ionization [23–28].

In the present experiment, we have studied a number of larger Na_n clusters ($n = 20,40,57,58,70$) interacting with an electron beam in the energy range of $\approx 0-5.5$ eV. As will be shown, the observed rise of low-energy cross sections and the strong increase in cross sections with cluster size provide a clear signature of polarization effects.

II. EXPERIMENT

The experimental geometry is outlined in Fig. 1. The supersonic beam of neutral clusters is produced by seeded expansion of sodium vapor through a small nozzle. The beam then passes through a skimmer and, following a 1.5-m-long flight path, passes through the collision region of the electron gun and continues towards the detector. There the clusters are photoionized by filtered UV light from an arc lamp, mass selected by a quadrupole mass analyzer (QMA), and registered by an ion counter.

Beam velocities were measured with the help of two identical fast (250 Hz) chopper wheels located ≈ 1.25 m apart: the mass spectrometer was set to a particular cluster size and the beam was alternately chopped by wheels 1 and 2. Cluster velocities can be read off directly from the time delay between the arrival of pulses from the two locations; they decreased from 1100 m/s for Na_{20} to 1015 m/s for Na_{70}.

The electron gun, as described before, [22], is based on the design of Ref. [29]. In the present case, electrons are emitted by an indirectly heated rectangular dispenser cathode (Spectra-Mat Inc., Watsonville, CA), extracted by a series of precision-aligned grids and masks, and intersect the cluster beam at a right angle inside an equipotential region bounded by two metal blocks. The length and height of the electron ribbon are $l = 25$ mm and $h = 1.4$ mm, respectively, and the entrance of the cluster beam into the collision region is defined by a 1.4×1.4-mm^2-square aperture. This ensures that the height of the cluster beam in the interaction region is the same as that of the electron beam. To prevent dispersal of the electron beam by space-charge effects, the gun assembly is mounted in a uniform magnetic field ($B = 1400$ G) which is directed parallel to the electron beam. Typical electron current densities in the interaction region were in the range of 800 μA/cm^2 at energies above 1 eV and up to 200 μA/cm^2 at energies below 0.5 eV, corresponding to total impact currents of $\sim 80-350$ μA. Retarding potential measurements were used to determine the electron gun energy resolution as well as the contact potential corrections to the electron energy. The resulting absolute electron energy calibration was estimated to be accurate to better than 0.1 eV, and the energy
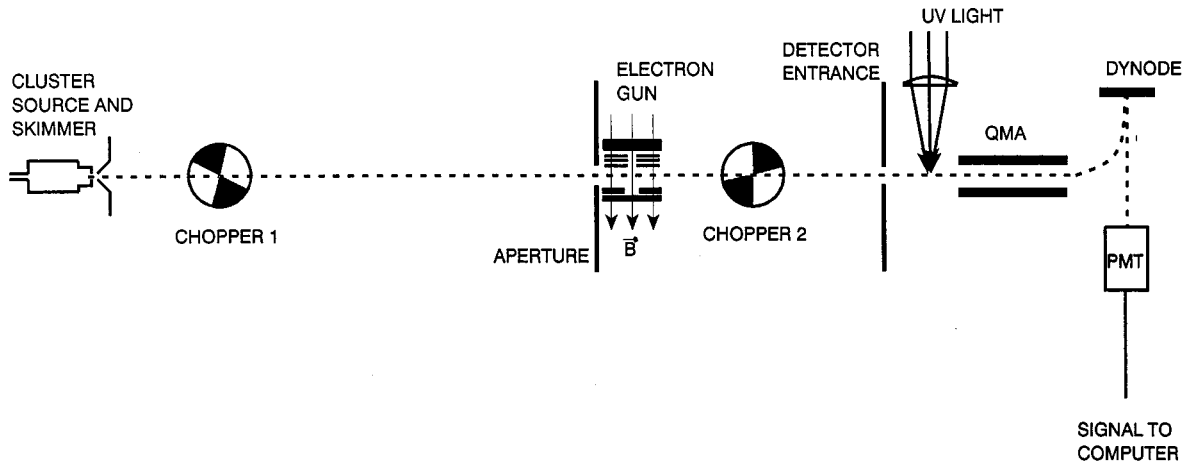
FIG. 1. Outline of the experimental arrangement (top view). The supersonic cluster source is operated at $T = 880$ K with argon carrier gas pressure of 6 bar. The nozzle and skimmer diameters are 0.075 and 0.4 mm, respectively; the nozzle temperature is maintained at $T = 1030$ K. The electron gun is located 1.5 m from the skimmer and 40 cm from the detector entrance. Collimating masks surrounding the electron gun collision region ensure full vertical overlap of the electron and cluster beams. The detector ionizing lamp is filtered to transmit light in the range of 240–410 nm (Kopp CS 7-54 glass). Cluster beam velocity is measured with the aid of two chopper wheels as described in the text. The electron beam is pulsed, and inelastic collisions result in a decrease in the cluster counting rate.

spread was approximately 0.3–0.4 eV full width at half maximum.

The electron-cluster interaction is monitored by setting the QMA to a chosen mass, pulsing the electron beam on and off at a rate of 4.77 Hz, and observing the concurrent depletion, ΔN, of the cluster counting rate on a multichannel scaler display. In our setup, the counting rates for individual clusters were in the range of $(1-5) \times 10^4$ per second, and the electron-induced depletion ratios were $\sim 0.2-1\%$. The cross section values discussed below are typically averages of two or three data points, with a total acquisition time of 30–45 min for each collision energy and cluster size. The estimated accuracy of the measurement is $\sim 10-20\%$.

The total effective interaction cross section σ_{eff} can be found from the following equation [30,31]:

$$\frac{\Delta N}{N} = \frac{\sigma_{\text{eff}} I_{\text{el}}}{v_{\text{cl}} h}, \qquad (1)$$

where N is the regular cluster counting rate, I_{el} is the electron number current, h is the height of the interacting beams (see above), and v_{cl} is the cluster beam velocity. This relation comes from considering how the electron beam scatters as it passes through the cluster beam. The velocity of the latter can be neglected during the scattering event, since the electrons move much faster. Thus the number of electronic collisions per unit time is proportional to the electron scattering cross section, the electron current, and the cluster beam density. Making use of the rectangular beam geometry and of the fact that the number of electron collisions is equal to the number of cluster collisions, one arrives at Eq. (1).

As the cluster masses are high and the collision energies low, a kinematic estimate shows that elastic electron scattering cannot lead to discernible cluster beam depletion. Thus the cross sections reported here must correspond to *inelastic* processes: cluster fragmentation and/or electron attachment. In the former case, the relative recoil of the fragments will remove them from the beam, as has been long observed in

photodepletion spectroscopy [32]. In the case of electron attachment, the resulting anions will be swept out of the beam by the electron gun's magnetic field. Even if this Lorentz force were absent, any long-lived anions would be removed from the beam by stray electric fields and by the potential barrier present at the entrance to the detector region.

The effective cross sections in Eq. (1) represent a convolution between the true energy-dependent electron scattering cross section, $\sigma(E)$, and the energy distribution of the electron flux, $I(E - E_0)$, where E_0 is the nominal collision energy. Thus

$$\sigma_{\text{eff}}(E_0) = \frac{\int_0^\infty \sigma(E) I(E - E_0) dE}{I_{\text{el}}(E_0)}, \qquad (2)$$

with the total electron current given by $I_{\text{el}}(E_0) = \int I(E - E_0) dE$. As mentioned above, the measured spread $I(E - E_0)$ in our experiment had approximately a symmetric Gaussian shape with a full width at half maximum of $\Gamma \approx 0.3$ eV for energies $E_0 \lesssim 1$ eV. For higher energies Γ increases to ≈ 0.4 eV, while at the lowest energies $I(E - E_0)$ is given an appropriate cutoff at $E = 0$. The convolution correction is, of course, most important at low collision energies. However, in our case it turns out to be relatively small: for the Langevin capture cross section σ_{cap} discussed in the next section, the strongest modification occurs between $E_0 = 0.1-0.3$ eV, where σ_{eff} is calculated to deviate from σ_{cap} by 10–20%.

We would like to emphasize a distinction between the experimental resolution of the nominal collision energy, E_0, and the width of the energy spread, Γ. As mentioned above and as will be illustrated in Figs. 2 and 3, the convolution-corrected cross section σ_{eff} still displays a strong energy dependence (discernible over a scale narrower than Γ [33]). Therefore it is informative to display individual data points measured for close-lying values of E_0 (which is determined
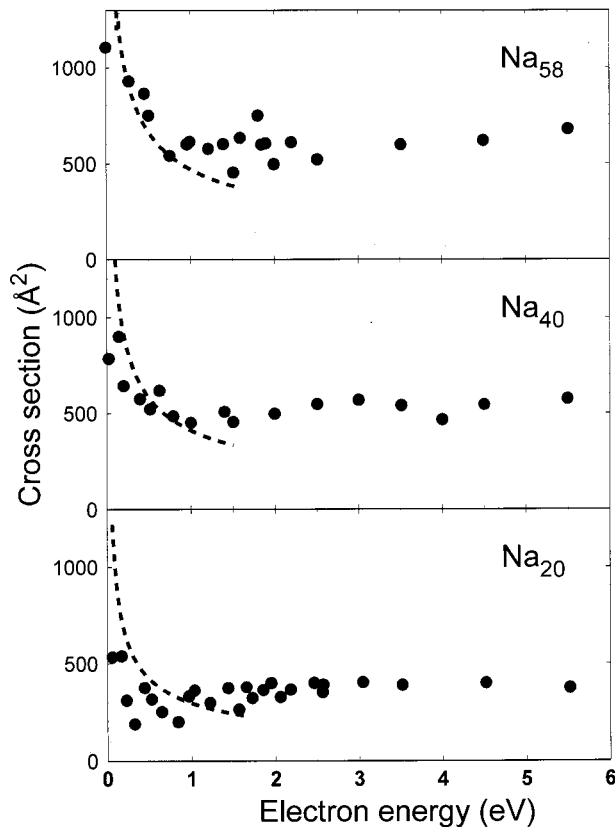
FIG. 2. Inelastic electron scattering cross sections for three clusters with closed valence electron shells vs nominal electron beam energy, E_0. Note the large magnitude of the cross sections. Dots, experimental results; dashed line, Langevin capture cross section convoluted with the electron gun energy spread. The estimated accuracy of the measured cross sections is $\sim$10–20%, and that of the absolute energy calibration is $\approx$0.1 eV.

to an accuracy of better than 0.1 eV). Similarly, it is appropriate to include data points acquired for values of E_0 below a few tenths of eV, as long as these are understood to represent cross sections properly averaged around these values. This representation is similar to that adopted, e.g., in Ref. [18], and permits a better-defined comparison with theoretical models than one would obtain from a coarse averaging of nearby data points.

III. RESULTS AND DISCUSSION

The results of the measurement are shown in Fig. 2 for three clusters with spherical closed electronic shells: Na_{20}, Na_{40}, and Na_{58}. Two features of the cross section curves can be immediately noticed. The inelastic cross sections increase with cluster size. Furthermore, they show a strong upwards trend for collision energies below 1 eV (''rise region'') and remain relatively flat at higher energies (''plateau region'').

A. Rise region

It is probably more than a mere coincidence that the transition region lies exactly in the range of cluster dissociation energies which are also $\approx$1 eV [34]. This means that in the rise region, direct electron-impact fragmentation is not possible, and one expects that electron attachment should be the

primary process. In fact, as stated in the Introduction, one may suppose that the electron capture process will be governed by the strong polarization field.

The origin of the polarization field is that a slow electron approaching a neutral cluster will polarize the latter and be subsequently attracted by the induced dipole field. For a perfect conducting sphere, this would correspond to the image charge potential [35]. For an isotropically polarizable target, such as a spherically symmetric cluster, the polarization potential seen by the incident electron is given by [2,36]

$$V_{\text{pol}} = -\frac{\alpha e^2}{2r^4}, \tag{3}$$

where α is the electric polarizability of the cluster.

In a classical picture of electron capture by the dipole polarization field, electrons approaching the cluster with impact parameters smaller than a certain critical value will spiral into the center of force and be captured. The corresponding classical capture cross section, known as the Langevin cross section, is given by [2,37]

$$\sigma_{\text{cap}}(E) = \left(\frac{2\pi^2 e^2 \alpha}{E}\right)^{1/2}, \tag{4}$$

where E is the energy of the incoming electron. A quantum-mechanical calculation [38] deviates from this result by no more than a few percent. We see explicitly that the high polarizability of metal clusters can lead to high electron attachment cross sections.

The dashed lines in Fig. 2 depict the capture cross sections calculated for the specific clusters studied here: the Langevin formula (4) convoluted with the experimental energy spread as described at the end of Sec. II. For Na_{20} and Na_{40}, we used the experimentally measured polarizabilities of sodium clusters [1,4]: $\alpha_{20} = 310 \, \text{Å}^3$, $\alpha_{40} = 590 \, \text{Å}^3$. No experimental values exist yet for the larger clusters, so for Na_{58} we took $\alpha_{58} = 770 \, \text{Å}^3$ as given by the analytical random-phase approximation (RPA) calculation described in [39]: this formalism provides results which are in good agreement with the available data for smaller sizes.

It is evident from the figure that the polarization capture mechanism provides an essentially quantitative representation of the low-energy cross section behavior for different cluster sizes. We would like to emphasize that the dashed lines employ no adjustable parameters. The very large values of the inelastic cross sections are seen to come from the strength of the long-range polarization potential.

We repeated the measurement on two open-shell clusters, Na_{57} and Na_{70} ($\alpha_{57} = 760 \, \text{Å}^3$, $\alpha_{70} = 920 \, \text{Å}^3$ [39]); the results are shown in Fig. 3. While the quality of the data is poorer due to the lower counting rate of these less stable clusters, the agreement with Eq. (4) is still satisfactory (the effects of nonsphericity should be washed out by orientational averaging). Overall, then, while the cross section measurement is challenging and the data are limited in energy resolution and scatter, there is an unequivocal accord between the variation of the cross sections with collision energy and cluster size and Eq. (4). This confirms that the Langevin mechanism dominates low-energy electron scattering for a wide range of cluster sizes.
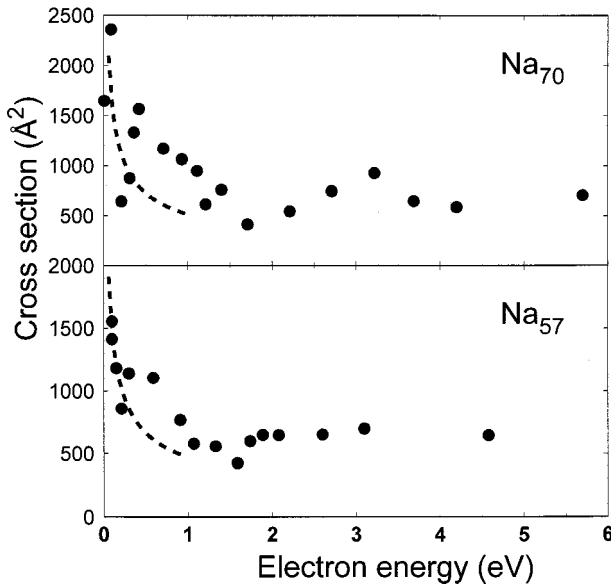
FIG. 3. Same as Fig. 2 for two open-shell clusters.

B. Plateau region

At higher energies (above ≈ 1 eV) other channels evidently come into play. The cross sections become approximately energy independent. The present level of resolution does not permit us to assign particular significance to any deviations from the average values that may be present in the data at these higher energies, although a detailed search for possible spectral features in this region is definitely a valuable goal.

Since the plateau region commences at energies just above the cluster dissociation threshold, it is reasonable to assume that here the main mechanism of beam depletion is cluster fragmentation. Indeed, it is known that electron bombardment leads to substantial fragmentation of alkali clusters [40]. However, it is not yet known whether this electron-impact fragmentation proceeds primarily directly, or via an intermediate electronic excitation such as a surface plasmon. In fact, calculations within the Born approximation in Refs. [26] and [27] suggested that low-energy electrons can excite multipole plasma resonances in clusters with significant cross sections. While the Born approximation itself cannot be quantitatively correct in this energy region, the large observed cross sections support the idea of a long-range inelastic excitation.

Indeed, assume that it is possible to associate the inelastic impact with a characteristic impact parameter b (that is, a characteristic interaction length). Then [22] one may rationalize the observation of a relatively flat cross section profile as follows: with angular momenta up to $L \approx kb$ contributing to the scattering process (k is the wave number of the incident electron), the upper bound to the inelastic scattering cross section turns out to be energy independent, and is given by [41]

$$\sigma_{mel}^{max} = \pi b^2. \qquad (5)$$

From the plateau regions of the spectra shown in Figs. 2 and 3, we can estimate the value of b, finding

$$b \approx (1.7-1.9)R, \qquad (6)$$

where $R = a_o r_s n^{1/3}$ is the conventional ion core radius of the Na_n cluster (a_o is the Bohr radius and $r_s = 4$ is the Wigner-Seitz radius of sodium). Such an estimate, while clearly schematic, does suggest that cluster excitation at these electron collision energies takes place at relatively large impact parameters. This is consistent with energy transfer proceeding via a long-range coupling to electronic excitations, rather than via a direct ''crash'' into the ionic core.

The threshold for excitation of collective resonances is the dipole surface plasmon frequency ($\approx 2.6-2.8$ eV for the Na cluster sizes studied here [39]), while the plateau region extends all the way down to the dissociation threshold, as noted above. Therefore other transitions, such as single-electron excitations, may be involved here. The associated cross sections, while large [23,27], are measurably smaller than those for collective resonance excitation, hence a theoretical analysis of the relevant channels in this energy range would be of interest. It is intriguing that the spectra suggest the presence of a broad minimum in the 1–1.5 eV energy range. In view of the energy resolution of our measurement, one may speculate that this region reflects an overlap between the channels of particle-hole excitation and Langevin capture.

Of course, further detailed experimental and theoretical investigations are required to unravel the exact dynamics of electron-impact fragmentation of metal clusters.

IV. CONCLUSIONS

We have measured absolute inelastic cross sections for low-energy electrons ($E \approx 0-5.5$ eV) interacting with neutral alkali clusters. The results can be summarized as follows.

(i) The cross sections are quite large, exceeding 1000 Å^2 at the lower energies. This signifies the action of strong long-range forces.

(ii) For collision energies below 1 eV, the cross sections rise strongly with decreasing energy, in quantitative agreement with the Langevin mechanism of electron capture by the polarization field. In other words, in this energy range the dominant process is electron attachment to the highly polarizable metallic cluster.

(iii) At energies exceeding ≈ 1 eV, cross sections become approximately independent of the collision energy. This behavior can be rationalized as reflecting efficient collision-induced cluster fragmentation. The associated impact parameters are found to be quite high, exceeding cluster radii by almost a factor of two. This implies that energy transfer here also proceeds via a long-range interaction, including the excitation of multipolar oscillations of the cluster electrons by the incoming charged particle.

These observations raise a number of basic questions related to electron dynamics near the surface of metal clusters. For example, what is the fate of the electrons that have been captured by the cluster polarization potential? In principle, they may spend some time in a metastable orbit outside the cluster core and autodetach or, more likely, transfer their energy to other cluster electrons and/or vibrational modes and ''fall'' into the cluster, resulting in fragmentation, ion-

ization, or radiation. The main relaxation mechanisms and the associated lifetimes are not known at present. Likewise, the precise channels of electron-cluster coupling at energies $\gtrsim 1$ eV remain difficult to understand theoretically as far as both electronic and ionic cluster degrees of freedom are concerned. Further experiments to study cluster anion formation, lifetime effects, and dissociation channels are currently underway in our laboratory.

[1] W. D. Knight, K. Clemenger, W. A. de Heer, and W. A. Saunders, Phys. Rev. B **31**, 2539 (1985).

[2] K. D. Bonin and V. V. Kresin, *Electric-Dipole Polarizabilities of Atoms, Molecules and Clusters* (World Scientific, Singapore, 1997).

[3] E. Benichou, R. Antoine, D. Rayane, B. Vezin, F. W. Dalby, Ph. Dugourd, M. Broyer, C. Ristori, F. Chandezon, B. A. Huber, J. C. Rocco, S. A. Blundell, and C. Guet, Phys. Rev. A **59**, R1 (1999).

[4] D. Rayane, A. R. Allouche, E. Benichou, R. Antoine, M. Aubert-Frecon, Ph. Dugourd, M. Broyer, C. Ristori, F. Chandezon, B. A. Huber, and C. Guet, Eur. Phys. J. D (to be published).

[5] V. V. Kresin, V. Kasperovich, G. Tikhonov, and K. Wong, Phys. Rev. A **57**, 383 (1998).

[6] V. V. Kresin, G. Tikhonov, V. Kasperovich, K. Wong, and P. Brockhaus, J. Chem. Phys. **108**, 6660 (1998).

[7] C. Guet, X. Biquard, P. Blaise, S. A. Blundell, M. Gross, B. A. Huber, D. Jalabert, M. Maurel, L. Plagne, and J. C. Rocco, Z. Phys. D **40**, 317 (1997).

[8] U. Näher, S. Bjørnholm, S. Frauendorf, F. Garcias, and C. Guet, Phys. Rep. **285**, 245 (1997).

[9] *Electron Collisions with Molecules, Clusters, and Surfaces*, edited by H. Ehrhardt and L. A. Morgan (Plenum, New York, 1994).

[10] O. Ingólfsson, F. Weik, and E. Illenberger, Int. J. Mass Spectrom. Ion Processes **155**, 1 (1996).

[11] M. K. Scheller, R. N. Compton, and L. S. Cederbaum, Science **270**, 1160 (1995).

[12] A. Chutjian, A. Garskadden, and J. M. Wadehra, Phys. Rep. **264**, 393 (1996).

[13] R. G. Keesee, A. W. Castleman, Jr., and T. D. Märk, in *Swarm Studies and Inelastic Electron-Molecule Collisions*, edited by L. C. Pitchford, B. V. McCoy, A. Chutjian, and S. Trajmar (Springer, New York, 1987).

[14] H. S. Carman, Jr., J. Chem. Phys. **100**, 2629 (1994).

[15] S. Matejcik, A. Kiendler, P. Stampfli, J. D. Skalny, A. Stamatovic, and T. D. Märk, Z. Phys. D **40**, 70 (1997).

[16] S. Matejcik, T. D. Märk, P. Spanel, and D. Smith, J. Chem. Phys. **102**, 2516 (1995).

[17] J. Huang, H. S. Carman, Jr., and R. N. Compton, J. Phys. Chem. **99**, 1719 (1995).

[18] A. A. Vostrikov, D. Yu. Dubov, and A. A. Agarkov, Tech. Phys. Lett. **21**, 517 (1995); A. A. Agarkov, V. A. Galichin, S. V. Drozdov, D. Yu. Dubov, and A. A. Vostrikov, Eur. Phys. J. D (to be published).

[19] D. Smith and P. Spanel, J. Phys. B **29**, 5199 (1996).

[20] J. M. Weber, M.-W. Ruf, and H. Hotop, Z. Phys. D **37**, 351 (1996).

[21] O. Elhamidi, J. Pommier, and R. Abouaf, J. Phys. B **30**, 4633 (1997).

[22] V. V. Kresin, A. Scheidemann, and W. D. Knight, in *Electron Collisions with Molecules, Clusters, and Surfaces* (Ref. [9]).

[23] M. R. Spinella, M. Bernath, O. Dragún, and H. Massmann, Phys. Rev. A **54**, 2197 (1996).

[24] M. R. Spinella, M. Bernath, and O. Dragún, Phys. Rev. A **58**, 2985 (1998).

[25] S. Keller, E. Engel, H. Ast, and R. M. Dreizler, J. Phys. B **30**, L703 (1997).

[26] L. G. Gerchikov, A. V. Solov'yov, J.-P. Connerade, and W. Greiner, J. Phys. B **30**, 4133 (1997).

[27] L. G. Gerchikov, A. N. Ipatov, and A. V. Solov'yov, J. Phys. B **30**, 5939 (1997).

[28] A. Ipatov, J.-P. Connerade, L. G. Gerchikov, and A. V. Solov'yov, J. Phys. B **31**, L27 (1998).

[29] R. E. Collins, B. B. Aubrey, P. N. Eisner, and R. J. Celotta, Rev. Sci. Instrum. **41**, 1403 (1970).

[30] B. Bederson and L. J. Kieffer, Rev. Mod. Phys. **43**, 601 (1971).

[31] R. E. Collins, B. Bederson, and M. Goldstein, Phys. Rev. A **3**, 1976 (1971).

[32] W. A. de Heer, Rev. Mod. Phys. **65**, 611 (1993).

[33] If the spectrum contains some sharp resonance peaks, it is clear that they cannot be resolved to any degree better than Γ (cf. discussion in Sec. III B). However, we are primarily interested in the low-energy capture cross section $\sigma_{cap}(E)$, Eq. (4). This is a steep monotonic function of energy, and calculation shows that even its convolution retains a strong dependence on the nominal collision energy E_0.

[34] C. Bréchignac, Ph. Cahuzac, J. Leygnier, and J. Weiner, J. Chem. Phys. **90**, 1492 (1988).

[35] J. D. Jackson, *Classical Electrodynamics*, 2nd ed. (Wiley, New York, 1975).

[36] E. W. McDaniel, *Atomic Collisions: Electron and Photon Projectiles* (Wiley, New York, 1989).

[37] L. D. Landau and E. M. Lifshitz, *Mechanics*, 3rd ed. (Pergamon, Oxford, 1976), Sec. 18.

[38] E. Vogt and G. H. Wannier, Phys. Rev. **95**, 1190 (1954).

[39] V. V. Kresin, Phys. Rep. **220**, 1 (1992).

[40] L. Bewig, U. Buck, C. Mehlmann, and M. Winter, J. Chem. Phys. **100**, 2765 (1994).

[41] N. F. Mott and H. S. W. Massey, *The Theory of Atomic Collisions*, 3rd ed. (Oxford University, Oxford, 1965), Chap. XII.